Early age fracture performance of 3D printable fiber reinforced cementitious composites

L. Esposito[1], M. Fioretti[2], M. Cucchi[3], F. Lo Monte[2], C. Menna[1], S. Moro[4], D. Asprone[1], and L. Ferrara[2]

ABSTRACT: The emerging digital manufacturing technologies, such as concrete 3D printing, require to pay specific attention to the "very early" and "early" performances of the employed cement-based materials, besides the "conventional" hardened state mechanical properties which are required to assess the structural serviceability and ultimate limit states of the intended applications. Indeed, it's clear that throughout the printing process, the development of the mechanical performances, from the very early stages, can significantly affect the structural build-up and discriminate about the successful accomplishment of the structural performance of the printed object. In this context, the present paper focuses on the early stage properties of a 3D printable fiber reinforced cementitious composite to be used in layered extrusion process. In particular, the development of the stress – strain constitutive behaviour under tensile and shear load conditions has been investigated as a function of the time. In a quality control framework, the development of tensile and shear fracture properties of the investigated materials, in the considered production time frame, is fundamental to discriminate about the printability of the mix, with reference not only to the quality of the finishing, but also to the spped of the printing process.

1 INTRODUCTION

Recent advances in digitally-based construction technologies have pushed towards the development of innovative materials and processing techniques. As a result, new concrete digital fabrication technologies, such as concrete 3D printing, focus the attention on the "very early" and "early" performances of cement-based materials rather than on "conventional" hardened state mechanical properties which are required to assess the structural serviceability and ultimate limit states of the intended applications.

Printable cement-based materials, like any other cementitious material, behave roughly as visco – plastic Bingham materials. They flow only when submitted to stresses higher than a critical threshold value τ_0 called yield stress (Roussel 2018). In the early stages (i.e. fresh state), the concrete material should have specific rheological properties in order to guarantee the so called "printability", which include the pumpability, extrudability and buildability requirements.

Because of the absence of a rigid mould when fabricating a 3D printed concrete object, high strength, high stiffness and thixotropic behaviour are required; moreover, in concrete layered extrusion, after fresh material deposition, each concrete layer must be able to carry its own self-weight and the weight of the layers above it. In particular, the yield stress τ_0 and plastic viscosity μ must be enough low during extrusion, but at the same time sufficiently high to allow the stability of the printed element. Another fundamental requirement for the printability is the tensile strength: if the printable cementitious paste doesn't have a sufficiently high tensile strength during the printing process, the extruded filament may break during the same extrusion process or undergo cracking because of the the development of shrinkage strains, restrained by the compatibility between

[1] *Department of structures for engineering and architecture, Università degli Studi di Napoli, Federico II*
[2] *Department of Civil and Environmental Engineering, Politecnico di Milano*
[3] *Laboratory for Testing Materials, Buildings and Structures, Politecnico di Milano*
[4] *BASF Construction Chemicals Italia*

subsequently extruded layers. In this framework, the experimental investigation on the mechanical behaviour of the material in its very early stages is fundamental to define the printability requirements and allow for the determination of final properties of the printed elements.

The measurement of τ_0 is generally performed using direct rheometric techniques that consist of slowly shearing the material and recording the peak shear stress required to initiate flow (Assaad et al. 2014).The direct shear test is an alternative test to traditional rheometric techniques and is widely used in soil mechanics to determine the cohesion C and angle of internal friction φ. This test can be used to evaluate the yield stress τ_0 of cement pastes. Good correlations between cohesion C and yield stress τ_0 were established by Assaad et al. (2014). Wolfs et al. (2018) have developed a numerical model to analyse the mechanical behaviour of fresh, 3D printed concrete based on Mohr – Coulomb failure criterion and linear stress strain behaviour up to the failure. The failure criterion was built through experimental results from to direct shear tests.

This paper reports on the early stage experimental investigation carried out on reference plain and fiber-reinforced cementitious printable mortars. The mechanical characterization concerns the tensile and shear load conditions and has been performed by adopting two specifics experimental set-ups, already employed by Lo Monte et al. (2019) to study the behaviour of highly flowable high performance fibre reinforced cementitious composites. In particular, for each load case, the tests were carried out considering different resting times of the samples, i.e. 30, 60 and 120 minutes, in order to study the development of the corresponding mechanical properties. In particular, the direct shear test was carried out without considering the influence of the normal load: the maximum stress value recorded during the test can be considered as an estimate of the cohesion.

The tests were carried out on two different mixtures. A first mix (i.e. the reference plain cementitious mix) was obtained using a cement-based mortar containing non-structural polypropylene fibers (indicated as “NSF” below). The second one (i.e. fiber-reinforced cementitious mix) was obtained by substituting the NSF with 0.45% in volume of structural Polyvinyl Alcohol Fibers (indicated as “SF” below). The percentage of SF was chosen as minimum value capable of providing a possible structural effect (as previously found for the same volume percentage of fibers [Wenlin L. and Jianping H. (2019), Yuexiu W. et al. (2018)], without changing the rheological requirements for printability. The comparison between the behaviour of the two mixtures is useful to evaluate if the structural fibers can provide a beneficial mechanical effect in the early stage of the printable mortars, whereas non-structural fibers (more flexible) are usually used to avoid plastic shrinkage cracking.

2 EXPERIMENTAL PROGRAM

2.1 The printable mortars

The printable mix used for the present experimental campaign is the same developed by some of the authors in [Asprone et al., 2018]. In details, the maximum aggregate size was selected at 4 mm, according to compatibility requirements with the 25 mm nozzle diameter. The water/cement ratio was tuned at 0.39. Non-structural polypropylene short fibers, shown in Figure 1(a) were also added to the mixture, at a dosage equal to 0. 12% by volume, in order to prevent plastic shrinkage cracking in the early curing stage and after the deposition process. A polycarboxylate superplasticizer was added to the mix in

order to improve the material pumpability. The slump class of the cementitious composite was evaluated according to the EN 12350–2:2009 procedure, the slump height loss being equal to 14 ± 2 mm, corresponding to workability class S1. The 28 days average cube strength R_{cm} was equal to 53.5 MPa.
As mentioned above, a second mix was obtained by substituting the non-structural fibers with a minimum percentage value in volume of structural fibers (indicated with "SF" below) - Polyvinyl Alcohol Fibers (see Figure 1b). A summary of the tests carried out in this study, i.e. direct tensile and shear tests, is reported in Table 1.
The mixing mode is the same as the one preceding the printing process.

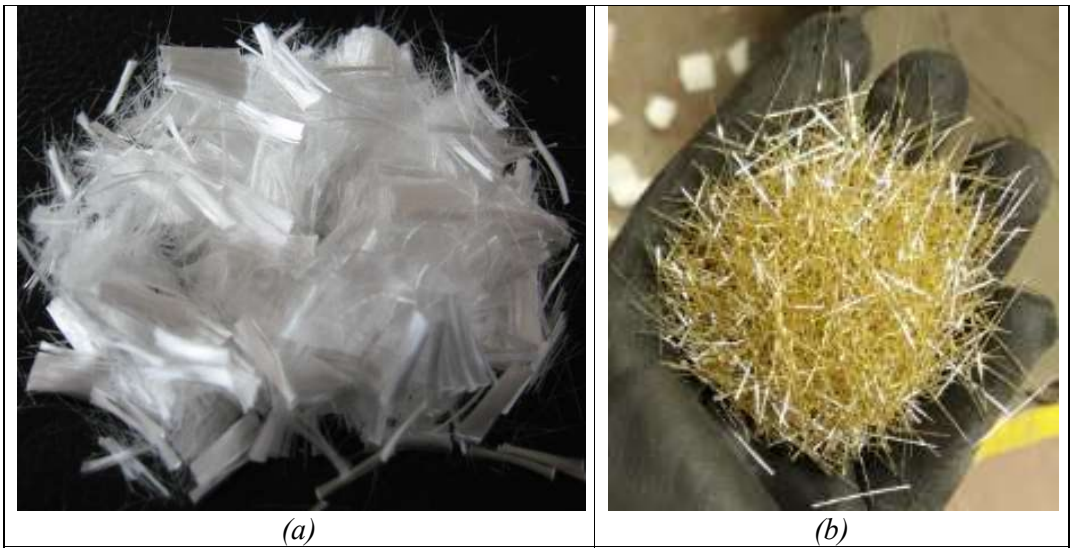

(a) *(b)*

Figure 1. (a) NSF - Polypropylene short fibers and (b) SF - Polyvinyl Alcohol fibers.

Table 1. Summary of tests - series "T" is for tensile test whereas "S" is for shear test

Sample	Resting time [min]	Mix
T30_NSF, S30_NSF	*30*	*0.12% NSF (non-structural fibers)*
T60_NSF, S60_NSF	*60*	
T120_NSF, S120_NSF	*90*	
T30_SF, S30_SF	*30*	*0.45% SF (structural fibers)*
T60_SF, S60_SF	*60*	
T120_SF, S120_SF	*90*	

2.2 Experimental test set-up

2.2.1 Tensile test

The set-up of the tensile test is shown in Figure 2. The sample is 332 mm long, 80 mm large and 60 mm high, with two semi-circular shaped recesses at the centre (cross section area reduction equal to 32.5%). The plexiglass box containing the sample consists of two parts, one fixed and the other movable. The movable part is attached to load cell and is free to slip, once the test has started. The friction force arising from the slipping surface was taken into account in the determination of the tensile force. The peculiar shape of the box allows the control of the position of the maximum stressed surface and, consequently, the approximate position of the crack, i.e. the cross section with the minimum resisting

area. The tensile force was applied through a load cell (with load capacity of 600 N), in displacement control condition. A constant horizontal displacement rate of 0.01mm/s was imposed on the mobile part of the box.

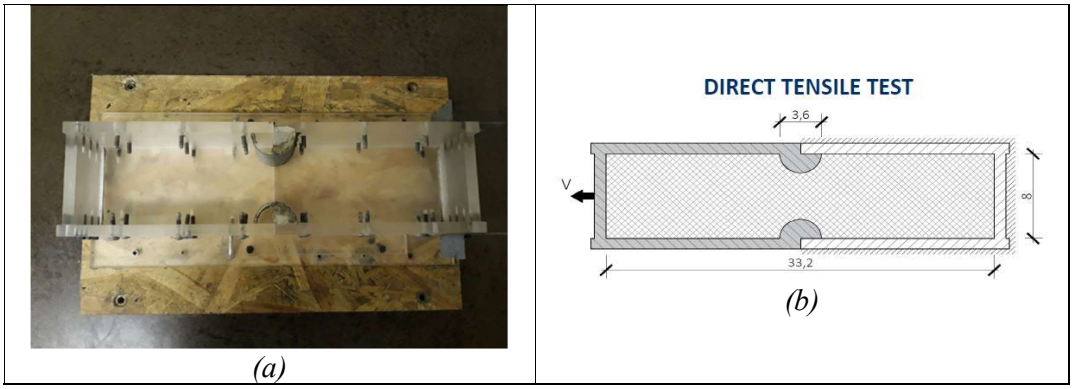

Figure 2. (a) Tensile Test Box and (b) sample dimensions (cm).

2.2.2 Shear box test

The schematization of the shear box test is shown in Figure 3a-b. The test is inspired by the direct shear test which is currently carried out on the soil in according to ASTM D3080. The sample sizes are shown in Figure 3(b). The test was carried out in displacement control, with a constant displacement rate of 0.1mm/s (imposed on the mobile part of the box, i.e. the bottom part in Figure 3(b)). The pure shear stress condition was assumed on the slippage surface between two parts of the sample.

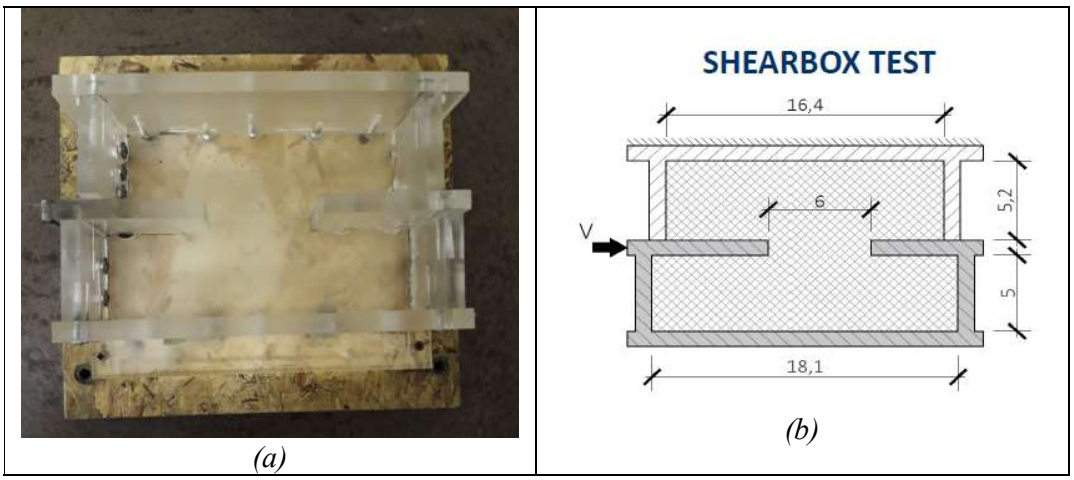

Figure 3. (a) Shear Box Test Set up and (b) Sample dimensions (cm)

3 EXPERIMENTAL RESULTS

3.1 Direct tensile test

In Figure 4, the tensile stress vs displacements curves (grey curves) are plotted for the reference plain cementitious mortar (i.e. with 0.12% by vol. NSF) for each sample and for each investigated resting time, i.e. 30, 60 and 120 minutes. The tensile stress values were obtained by dividing the force recorded through the load cell by the "ligament"

cross-sectional area of the specimen, equal 2640 mm^2. As remarked above, the friction effect (experimentally quantified equal to about 10N) was taken into account in this calculation by subtracting the corresponding force from the total recorded one.

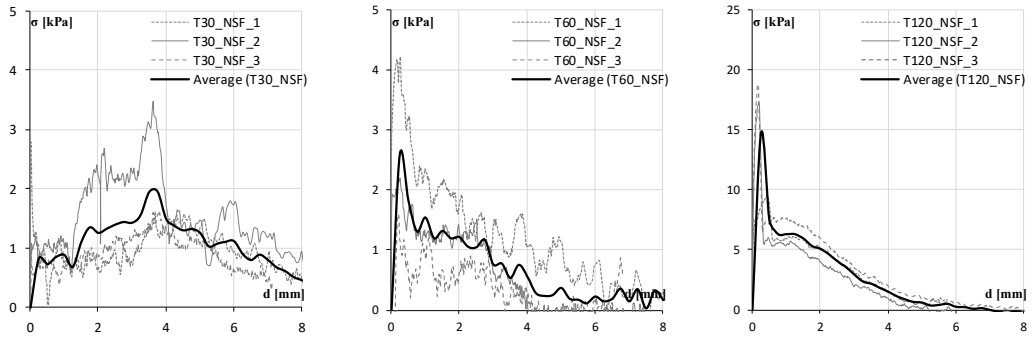

(a) *(b)* *(c)*

Figure 4. Displacement- tensile stress curves at (a) 30 minutes, (b) 60 minutes and (c) 120 minutes (with 0.12% of NSF) - a different scale of representation is adopted in (c).

Figure 4 also shows that the dispersion of the stresses is greater for shorter resting times (i.e. 30 and 60 minutes). In particular, it is quite difficult to identify the value of tensile strength at 30 minutes, the "shape" of the constitutive law being not well definable. The behaviour changes at 60 minutes, with the onset of fluid-to-solid transition, even if the dispersion remains quite high. At 120 minutes the transition from fresh to solid-like material behaviour appears to be completed and the recorded behaviour is typical of quasi-brittle cementitious materials. The maximum average tensile strength is equal to 2.0, 2.6 and 15.0 kPa at 30, 60 and 120 minutes from the casting respectively.

A second set of tests was carried out on the fiber reinforced cementitious mix defined about containing 0.45% by volume of structural PVA fibers. In Figure 5, the tensile stress vs displacement curves for each resting time are plotted. Also in this case it is possible to observe a transition from plastic (fluid) to brittle (solid) behaviour with increasing time. As a matter of fact, the fluid to solid transition looks like to be quite well defined, with reduced scattering, already at 60 minutes, whereas in the previously investigated mix it likely took some longer time to be completed. The maximum average tensile strength is 1.0, 3.5 and 7.0 kPa, respectively for 30, 60 and 120 minutes from the casting.

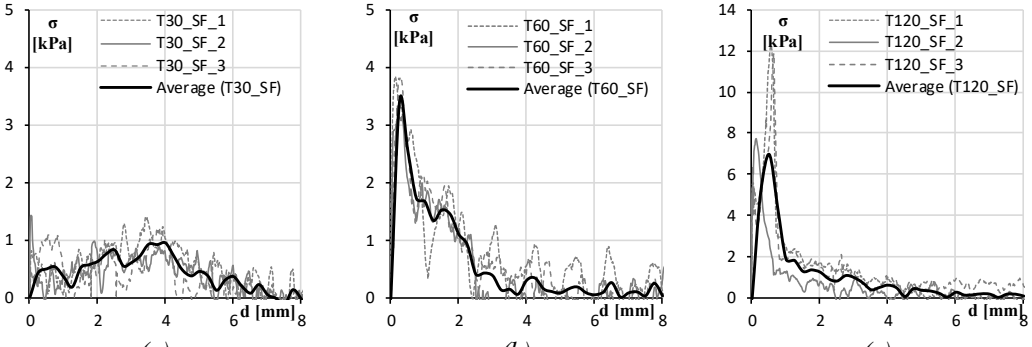

(a) *(b)* *(c)*

Figure 5. Displacement- tensile stress curves at (a) 30 minutes, (b) 60 minutes and (c) 120 minutes (with 0.45% of SF) - a different scale of representation is adopted in (c)

The average curves of the two mixture are plotted and compared in Figure 6(a). The comparison shows that the substitution of NSF with SF resulted in a decrease in the average maximum tensile stress, particularly at 120 min. The different behaviour can be explained considering several factors. First of all, it is worth remarking that specimens employed in this investigation were not "extruded" but manually fabricated by "plastering" the quite stiff (extrudable) mixes into the moulds. This may have affected the dispersion of the fibers, also with reference to their different stiffness: the NSF are more deformable than the SF ones and they may have better adapted to the mould filling procedure, being thus better dispersed and able, in the very early investigated ages, to better follow the deformation of the surrounding mortar. In this sense they may have been able to provide a better pull-out response, which has resulted into a higher strength. Moreover the NSF, being shorter and thinner than the SF ones (see Figure 1 (a) and (b)), are greater in number. This may contribute to explain not only the higher measured tensile strength but also the higher post-cracking residual stress retention capacity (see the different shape of the softening branches of dashed and continuous curve at 120 min in Figure 6(a)).
Figure 6(b) shows the tensile failure and crack pattern of a sample at 120 minutes from casting (a similar crack pattern was observed for each tested sample).

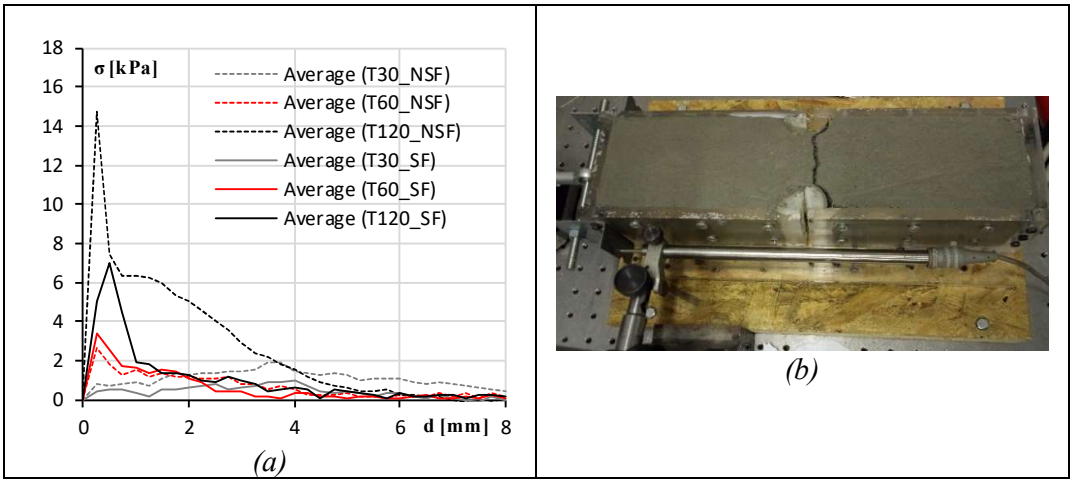

Figure 6. (a) Comparison of the average curves for 30, 60 and 120 minutes from the casting; (b) Tensile failure of the sample at 120 minutes from casting (with NSF).

3.2 Direct shear box test

In Figure 7 and 8, the tangential stress vs slip curves (grey curves) are plotted for the both the investigated fiber reinforced cementitious mixes (with 0.12% NSF and 0.45% SF respectively) and for all the analyzed resting time, i.e. 30, 60 and 120 minutes. Also in this case, a fluid to solid transition can be observed to occur which is also likely to correspond to a transition between two different resistant mechanisms. A first mechanism is linked to the material shear strength in correspondence of the "ligament" between the two parts of the specimen. This leads to the formation of crack inclined at 45°stating from the notch tips (see Figure 9). A second resistance mechanism takes over after cracking and is characterized by the formation of an inclined strut, which makes the stress to further increase after the shear cracking, up to a peak value, after which a sudden stress drop accompanied by the shearing off of the ligament cross section occurs (see Figure 7 (a-b)-

8(a-b) and 9(a-b)). At higher resting times (i.e. 120 minutes) the response changes, which attainment of a peak strength followed by a quasi-plastic response. It is likely that the increase of the tensile, and hence of the shear cracking, strength counteracts the propagation of the inclined shear cracks, which remain quite "limited", and hence the formation of the compressed strut in between, in favour of a shearing off of the ligament cross section (see Figure 9(c)), as also typical of the response of push-off specimens in hardened concrete (Barragan et al., 2006).

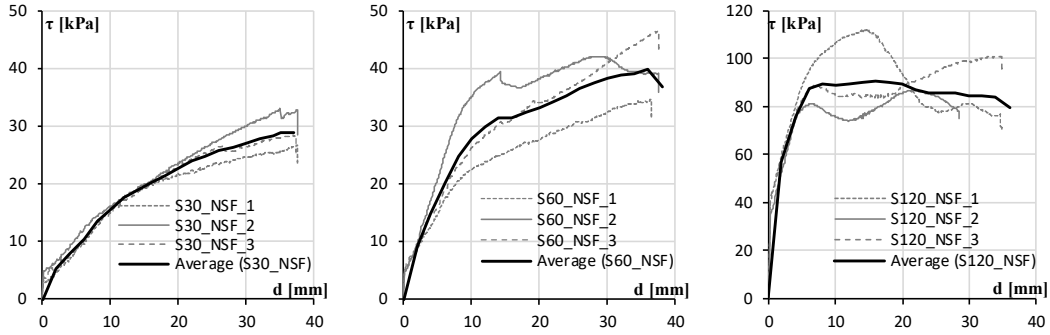

(a) *(b)* *(c)*

Figure 7 shear stress vs slip curves at (a)30 minutes, (b)60 minutes and (c)120 minutes (with 0.12% of NSF) - a different scale of representation is adopted in (c).

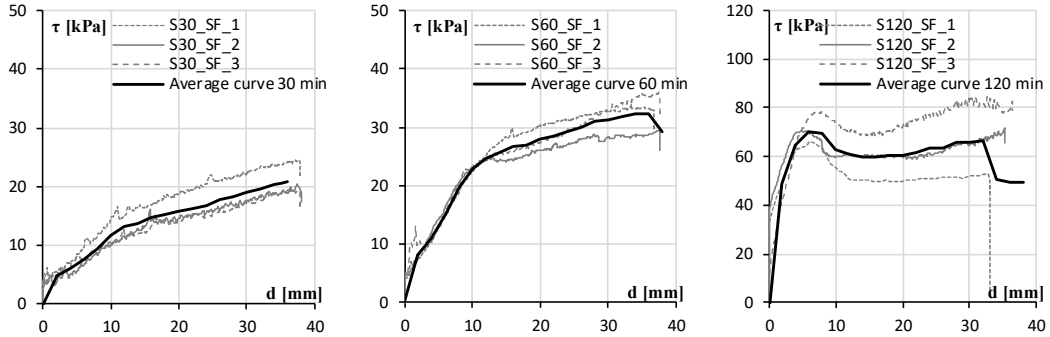

(a) *(b)* *(c)*

Figure 8. shear stress vs slip curves at (a)30 minutes, (b)60 minutes and (c)120 minutes (with 0.45% of structural fibers) - a different scale of representation is adopted in (c).

(a) *(b)* *(c)*

Figure 9. Shear Test: crack pattern at (a) 30 minutes, (b) 60 minutes and (c) 120 minutes (with NSF).

In Figure 10(a) the strength average curves are plotted: the mix with 0.12% of NSF shows a higher resistance than mix with 0.45% of SF, coherently also with what analysed above with reference to tensile strength, the same reasons being held as responsible.

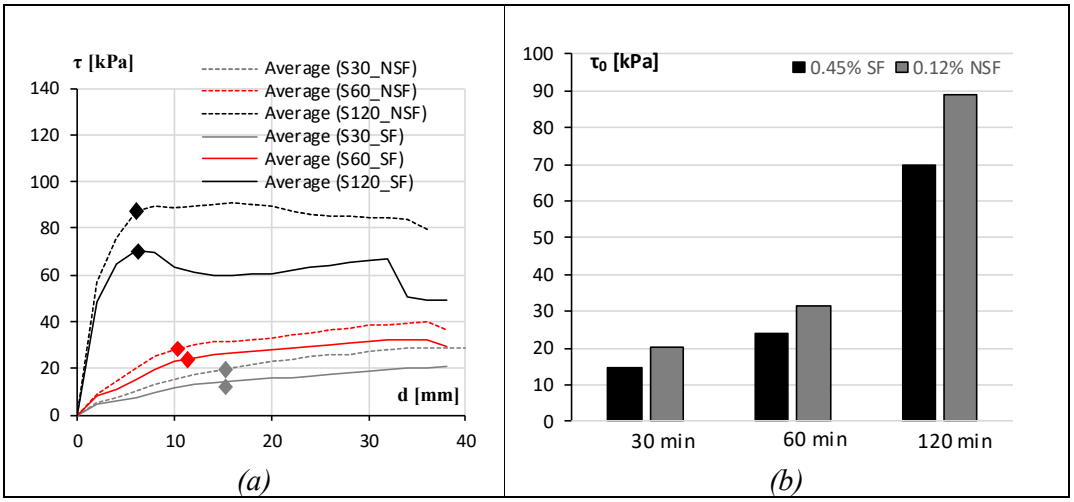

Figure 10. Shear Test: (a) Comparison of the average curves for 30, 60 and 120 minutes from the casting; (b) Yield stress vs Time.

In order to analyse the evolution with time of the mechanical performance of both the investigated composites the value of the shear stress at the slope change of the shear stress vs slip curves has been selected as a representative parameter (see the diamond symbol in Figure 10(a)) and its evolution with time is shown in the Figure 10(b). This data, also fitted through an exponential law, have been compared with the laws proposed by Roussel (2005) and Perrot et al. (2015).

Roussel proposed the following linear law:

$$\tau_0(t) = \tau_{0,0} + A_{thix} t \quad (1)$$

where $\tau_{0,0}$ is the yield stress of the material at zero rest time and A_{thix} is the structuration rate. Perrot et al. (2015) proposed an exponential law, which converges to the linear by Roussel over short resting rimes:

$$\tau_0(t) = \tau_{0,0} + A_{thix} t_c \left(e^{t_{rest}/t_c} - 1\right) \quad (2)$$

where t_c is a characteristic time, the value of which is chosen in order to obtain the best fit with experimental data.

The comparison between experimental data and analytical model is shown in Figure 11. The parameters of the analytical models were calibrated in order to have the best fit with experimental data. The same structuration rate A_{thix} was assumed for both mixtures (i.e. 0.39 kPa/min), since its value is related to the chemical reaction in the cement paste. The parameter values used in the Perrot and Roussel models are given in Table 2. The obtained agreement, though providing comfortable evidence about the reliability of the proposed mechanical parameter as representative of the time evolution of the material behaviour, obviously needs further investigation in order to find the exact correlation between the shear strength obtained by direct shear test and the rheological yield stress value.

Table 2. Parameter values used in Roussel and Perrot laws

Mix	A_{thix} (kPa/min)	$\tau_{0,0}$ (kPa)	t_c (min)
0.12% SF	*0.39*	*2.5*	*170*
0.45% NSF	*0.39*	*7.5*	*120*

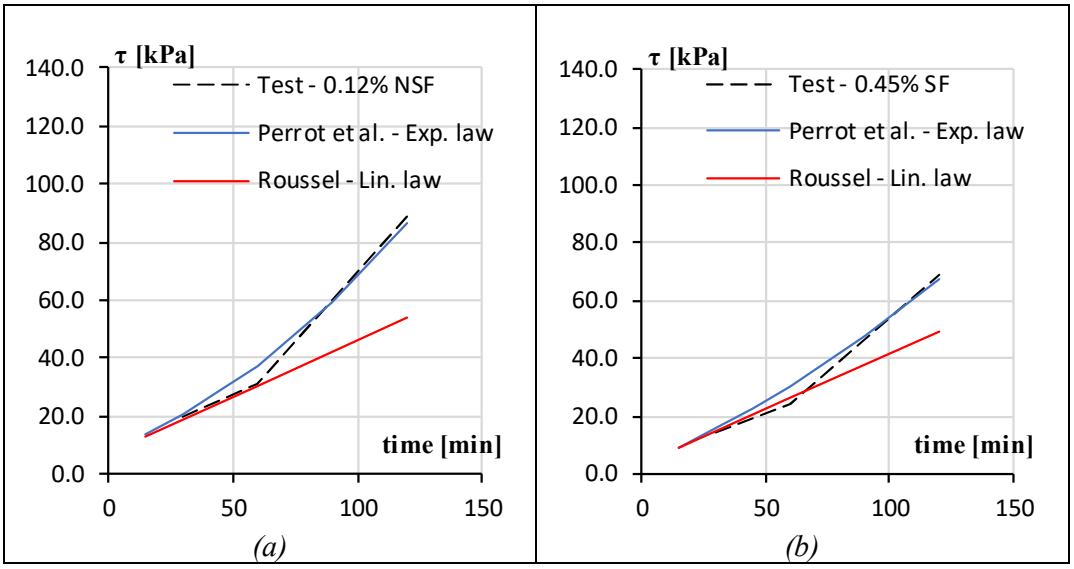

Figure 11. Evolution of the yield stress: Test VS Analytical Model (a) mix with 0.12% of NSF (b) mix with 0.45% of SF.

4 CONCLUSIONS

In this paper, the early age properties of two different printable mortars, reinforced with 0.12% by volume of non-structural polypropylene and 0.45% by volume of structural polyvinyl-alcohol fibers have been studied. Direct tensile tests and direct shear tests have been carried out for different value of the resting time (i.e. 30, 60 and 120 minutes from casting), in order to define the time evolution of the mechanical behaviour with the final purpose of identifying a suitable mechanical parameter able to characterize such evolution and provide.

The tests have shown that:

- as resting time increases, a transition from fluid to solid behaviour can be clearly identified. In the case of tensile tests this is evident with the onset of elastic-softening behaviour, typical of quasi brittle materials, whereas in the case of shear tests a transition from a mixed-mode (inclined shear crack + strut) fracture towards a shear fracture has been observed;
- for the investigated fiber volume fraction the fibres are not able to modify the post-cracking response of the material, which remains softening; though, the interaction between the specimen production methods and they fiber type may have affected fiber effectiveness and determined different values of the measured tensile and shear strength;
- a preliminary time evolution law of a shear stress parameter was obtained thanks to the direct shear test results, and correlated with remarkable agreement with laws available in the literature for thixotropic evolution of rheological parameters (which may confirm the nature of the phenomena responsible of the measured evolution of

the mechanical behaviour of printable fiber reinforced cementitious composites in their very early age). The need has been also highlighted of further investigating this aspect in order to find the exact correlation between the shear strength obtained by direct shear test and the yield stress values obtained from rheological tests.

Further investigation on mix with higher dosage (i.e. 1 – 2 % in volume) of structural fibers will be carried out, in order to study the possible improvement of mechanical behaviour, without affecting the printability requirements.

REFERENCES

Asprone, D., Auricchio, F., Menna C. and Mercuri, V. (2018). 3D printing of reinforced concrete elements: Technology and design approach. *Construction and Building Materials*. V. 165, 218–231.

Assaad, J.J., Harb, J. and Maalouf, Y. (2014). Measurement of yield stress of cement pastes using the direct shear test. *Journal of Non-Newtonian Fluid Mechanics*, V. 214, 18-27.

Barragan, B., Gettu, RE., Agullo, L. and Zerbino, R. (2006). Shear failure of steel fiber-reinforced concrete based on push-off tests. *ACI Materials Journal,* V. 103(4), 251-257.

Lo Monte, F., Zago, G., Cucchi, M. and Ferrara, L. (2019). Correlation between "very early" age fracture performance and evolution of rheological properties of high performance fiber reinforced cementitious composites with adapted rheology. *9th International RILEM Symposium on Self Compacting Concrete (SCC9) and 2nd International RILEM Conference on Rheology and Processing of Construction Materials (RheoCon2)*, Dresden, 8-11 September (2019).

Perrot A., Pierre A., Vitaloni S. et al. (2015). Prediction of lateral form pressure exerted by concrete at low casting rates. *Materials and Structures*, V. 48, no. 7, 2315–2322.

Roussel N. (2005) Steady and transient flow behaviour of fresh cement pastes. *Cement and Concrete Research*, V. 35, 1656-1664.

Roussel N. (2018) Rheological requirements for printable concretes. *Cement and Concrete Research*, V. 112,76-85.

Wenlin L. and Jianping H., (2019). Experimental investigation on compressive toughness of the PVA-steel hybrid fiber reinforced cementitious composites. *Frontiers in Materials*, V. 6, Article 108.

Wolfs, R.J.M., Bos, F.P. and Salet, T.A.M. (2018). Early age mechanical behaviour of 3D printed concrete: Numerical modelling and experimental testing. *Cement and Concrete Research*, V. 106, 103-116.

Yuexiu W., Wanpeng S., Wusheng Z., and Xianjun T. (2018). An experimental study on dynamic mechanical properties of fiber-reinforced concrete under different strain rates. *Applied sciences,* V. 8, 1904.